Protein aggregation, water binding and thermal gelation of salt-ground hake muscle in the presence of wet and dried soy phosphatidylcholine liposomes

Marín, D., Alemán, A., Montero, P., and Gómez-Guillén, M.C.*

Institute of Food Science, Technology and Nutrition (ICTAN-CSIC)

José Antonio Novais 10, 28040 Madrid (Spain)

*Author for correspondence: mc.gomez@csic.es

Abstract

Different soy phosphatidylcholine liposomal preparations (fresh, high-pressure-treated, frozen-thawed, freeze-dried and spray-dried) were incorporated in salt-ground hake (*M. merluccius*) muscle and their effects on protein aggregation, water binding and thermal gelation were studied. Hydrodynamic properties of liposomes varied within the range of 123 to 507 nm for particle size and –40 to –49.5 mV for zeta potential. Addition of liposomes to the salt-ground muscle decreased protein solubility and increased water holding capacity, regardless of the vesicle particle size or membrane surface charge. Liposomes caused an increase in protein thermal stability, as observed by DSC, and also increased the spacing between myofibrils, leading to more water trapped within the myofibrillar protein network, as revealed by the LF-NMR-^{1}H study. The presence of liposomes slightly modified the viscoelastic behaviour and interfered with the thermal aggregation of muscle proteins, the mechanisms for this interference being different depending on the type of liposome preparation (wet or dry form). The present work suggests the possible use of a highly appreciated fish species, which could be subjected to landing obligation under Total Allowable Catch regulations (EU), for the development of a high-added-value fish product functionalized by the addition of liposomes.

Keywords: hake mince, protein aggregation, water binding, thermal gelation, dried liposomes, soy phosphatidylcholine.

1. Introduction

Hake (*Merluccius merluccius*) is one of the most important demersal fish stocks in European waters, being found in the Mediterranean Sea, the North Sea, and the eastern Atlantic Ocean. It can commonly be caught in mixed fisheries along with cod, haddock and whiting; therefore it could be considered as targeted catch and also as by-catch. From 1st January 2015, EU Regulation No 1380/2013, approved by the European Parliament as part of a Common Fisheries Policy for the conservation and sustainable exploitation of fisheries resources, has started to implement the landing obligation for commercial fisheries under Total Allowance Catch (TAC) or under minimum landing size (MLS) in European waters and for European vessels fishing in the high seas. Discarded fish cannot be used for direct human consumption; however, an appropriate transformation into gel-based fish products would represent an economically profitable use of these resources. Previous studies about the use of hake mince for producing restructured fish products have been carried out with other species of lower commercial value, such as *M. productus* (Zhou & Li-Chan, 2009) or *M. capensis* (Cardoso, Mendes, Pedro & Nunes, 2008). European hake is a highly appreciated fish species with a high economic value which is commonly consumed in the form of fresh or frozen fillets or slices. For specific situations in which the established quota for hake fishing has been exceeded, the excellent gel-forming capacity of the muscle protein of this species could be used to obtain healthy products with high added value (Moreno, Borderías & Barón, 2010; Martelo-Vidal, Guerra-Rodríguez, Pita-Calvo & Vázquez, 2016). The light colour, low fat content and smooth flavour of hake mince are desirable characteristics for the development of gel-based functional fish products by incorporating specific nutrients and bioactive compounds. Encapsulation of

49 bioactive compounds in liposomes could be a way of enhancing their efficacy and their
50 resistance to chemical or physical degradation in food systems (Mozafari, Johnson,
51 Hatziantoniou & Demetzos, 2008; Da Silva Malheiros, Daroit & Brandelli, 2010). Liposomes are
52 amphipathic spherical colloidal vesicles whose structure is based on an aqueous inner space
53 surrounded by one or more phospholipid bilayers, allowing entrapment of both hydrophilic
54 and hydrophobic substances. Liposomes can be prepared from a variety of lipids. The use of
55 partially purified soy phosphatidylcholine for food-grade liposome production would provide
56 nutritional value owing to its high polyunsaturated fatty acid composition and residual
57 tocopherol content (Taladrid et al., 2017). Furthermore, the addition of non-synthetic
58 phospholipids does not raise any food legislation concerns (Laye, McClements & Weiss, 2008).
59 Freeze-dried soy phosphatidylcholine liposomes loaded with various bioactive compounds
60 were found to reduce the gel strength of surimi squid gels and to maintain their stability during
61 long-term frozen storage. Furthermore, the digestibility of the weaker gel matrices was
62 enhanced as a result of distortion of protein-protein interactions resulting from the presence
63 of liposomes (Marín, Alemán, Sánchez-Faure, Montero & Gómez-Guillén, 2018).

64 Aqueous liposome suspensions are stable for a limited time, after which adverse events may
65 take place, such as hydrolysis, liposome aggregation, phospholipid oxidation and drug leakage.
66 To improve their stability several technological methods could be applied, such as freezing
67 (Chen, Han, Cai & Tang, 2010), freeze-drying (Sebaaly, Greige-Gerges, Stainmesse, Fessi &
68 Charcosset, 2016) or spray-drying (Gültekin-Özgüven, Karadağ, Duman, Özkal & Özçelik, 2016),
69 which could be combined with the addition of cryoprotectants in order to protect the bilayers
70 against freezing- or freeze-drying-induced damage (Stark, Pabst & Prassl 2010). High
71 hydrostatic pressure (HHP) is a cold pasteurization technique which has already been
72 implemented in the food industry. It is also a feasible industrial process for preservation and
73 decontamination of drug delivery systems (Rigaldie et al., 2003).

There is no available information regarding the influence of the hydrodynamic particle properties and physical presentation (wet or dry state) of liposomes on fish muscle protein thermal aggregation. This would be an important point for designing a functional fish gel product with desirable sensory and technological properties.

The aim of this work was (i) to evaluate the impact of different stabilization treatments (high pressure, freezing, freeze-drying and spray-drying) on the properties of soy phosphatidylcholine liposomes, and (ii) to study the effect of adding different types of liposomal preparations on the water binding, protein aggregation and gelling properties of salt-ground hake muscle as a model system for developing functional gel-like fish products. At the same time, this approach will be also useful to valorise hake from eventual discards.

2. Materials and Methods

2.1. Preparation of liposomes

Partially purified phosphatidylcholine (PC) was obtained by dissolving commercial soybean lecithin (Manuel Riesgo S.A., Madrid, Spain) in ethyl acetate (1:5, w/v) and subsequently performing five washes with acetone. The preparation and chemical characterization of the partially purified phosphatidylcholine used in the present study was described in a recent work (Taladrid et al., 2017). Briefly, phospholipids represented ≈95% of total lipids in PC, the most abundant fatty acids being, in descending order, linoleic (C18:2n6c), palmitic (C16:0), oleic (C18:1n9c), linolenic (C18:3n3) and stearic acid (C18:0). Phosphatidylcholine was markedly the most abundant phospholipid class, followed by phosphatidylethanolamine, as well as low amounts of lyso forms of phosphatidylcholine and phosphatidylethanolamine, phosphatidylinositol and phosphatidic acid. Trace amount of aminoacids and tocopherol were also reported. The PC powder was stored at –20 °C until use.

Liposome dispersions in 0.2 M phosphate buffer (pH 7) were prepared according to Marín et al. (2018). Glycerol was added to some formulations in a proportion of 0.6 mL per g of PC. All dispersions were vortexed at 60 °C to produce multilamellar vesicles, and subsequently sonicated (probe tip) at a measured power of 120 W for 5 minutes, with a 60 s stop every min to allow sample cooling.

2.2. Stabilization of liposomes

Fresh liposome dispersion with no technological treatment was used as a control sample (L). The liposome dispersion was subjected to high pressure treatment using a Stansted Fluid Power Iso-lab 900 High Pressure Food Processor (Model: FPG7100:9/2C, Stansted Fluid Power Ltd., Harlow, Essex, UK) at 600 MPa for 20 min at 20 °C in one cycle. The pressurized liposome dispersion was designated as HP sample and was stored at 4 °C until use (1–2 days). Freeze-thawed liposomes, without and with glycerol (FT and FT-G, respectively) were obtained by freezing liposomal dispersions at –20 °C for 24 h, and then they were thawed and stored at 4 °C until use (1–2 days). Freeze-dried samples were prepared without and with glycerol (FD and FD-G, respectively). The freeze-drying process was performed by placing 50 mL of newly prepared liposomal dispersion in 100 mL plastic cups with perforated caps, which were frozen at –80 °C for 24 h. Lyophilization took place in a VirTis Freeze Drying unit (VirTis mod.6K TEL-85, coupled to a TRIVAC-E2 pump) operating at a vacuum level of 0.13 mbar, with the collector starting at a temperature of −45 °C and reaching –80 °C after 48 h. The atomized sample (SD) was obtained by spray-drying (BÜCHI, Mini Spray Dryer B-290, Switzerland) under the following conditions: Inlet Temperature 170 °C, Outlet Temperature 89 °C, Aspirator 70%, Pump 20%, Q-Flow 45 mm.

All liposome dispersions were concentrated by centrifugation at 4000 *g* for 1 h at 2 °C (Multifuge 3 L-R, Heraeus, Madrid, Spain) using centrifugal filters (Amicon® Ultra-15, Ultracel® -3K, Merck Millipore Ltd., Tullagreen, Carrigtwohill, County Cork, Ireland).

2.3. Characterization of liposomes

Particle size, polydispersity index and zeta potential of liposomes were determined using a Zetasizer Nano ZS (Malvern Instruments Ltd., Worcestershire, UK). Z-average and polydispersity were measured by dynamic light scattering (DLS) and zeta potential was measured by laser Doppler velocimetry through the electrophoretic mobility, provided by the Huckel approximation. All samples were diluted in 0.2 M phosphate buffer at pH 7.0 to avoid particle aggregation. At least 10 replicates were measured per sample. Dried liposomal preparations were previously rehydrated by dispersing in distilled water at 0.77 mg/mL for 30 min at 20 °C under magnetic stirring.

The moisture content was determined according to Marín et al. (2018). For the determination of the dispersibility in water, both the liposome dispersions and the dried liposomal preparations were mixed with distilled water (1 % w/v) under agitation (100 rpm) at 20 °C for 150 min and centrifuged at 3500 rpm (Multifuge 3 L-R, Heraeus, Madrid, Spain) for 5 min. The supernatant was dried at 105 °C for 24 h and weighted. The dispersibility in water was calculated by weight differences with respect to the dry matter content originally present in each sample preparation, and was expressed as a percentage. Determinations were carried out in triplicate.

2.4. Preparation of salt-ground muscle systems and gels

Fresh European hake (*M. merluccius*) fillets were purchased in a local market. Chopped muscle (150 g) was homogenized with 1% NaCl and 75 mL of each concentrated liposome dispersion (L, HP, FT and FT-G) in a beater surrounded by ice for 2 min. On the other hand, 150 g of chopped muscle was also homogenized with 1% NaCl and with a weighted amount of each dried liposomal preparation, namely 4.69 g of FD, 6.48 g of FD-G and 6.47 g of SD, in a beater for 1 min; then distilled water was added to complete a liposomal volume of 75 mL and it was

beaten again for 3 min. Additional water was incorporated in order to adjust the final moisture content in all the salt-ground muscle samples to the same level, so that both wet and dried liposomal preparations represented the same dry weight in the muscle formulation. A control salt-ground muscle batch without liposomes (M) was prepared by adding 75 mL of water to the formulation. The salt-ground muscle model systems were stored at 4 °C until use.

The gels were prepared by stuffing the resulting pastes into 35 mm plastic cellulose casings (Viscase SA, Bagnold Cedex, France), and heating in a Rational oven (Combi-Master CM 6) at 60 °C and 80 °C for 45 min. After thermal treatment, the gels were dipped into ice water to cool them quickly and stored overnight at 4 °C.

2.5. Characterization of salt-ground muscle systems

2.5.1. Water content, soluble protein and water holding capacity

Moisture content was determined according to method 950.46 (A.O.A.C., 2005). For determination of soluble protein, the salt-ground muscle (without or with liposomes) was further homogenized with sodium chloride (5 % w/v) in a proportion of 1:25 (w/v) using an Omni-Mixer model 17106 homogenizer (Omni Intl., Waterbury, Conn., USA) surrounded by ice for 1 min. The resulting homogenates were stirred at 4 °C for 30 min and then centrifuged at 6000 g for 30 min at 4 °C. Total protein content was determined in the supernatant (soluble protein) and in the hake muscle (total protein) with a LECO-FP 2000 nitrogen/protein analyser (LECO Corp., St. Joseph, MI, USA) using a nitrogen-to-protein conversion factor of 6.25. Soluble protein content was expressed as the percentage of soluble protein with respect to total protein originally present in the hake muscle. The water holding capacity (WHC) was determined using the centrifugation method described by Gómez-Guillén, Montero, Hurtado and Borderías (2000). Determinations were carried out at least in triplicate.

2.5.2. SDS-polyacrylamide gel electrophoresis (SDS-PAGE)

173 The electrophoresis of soluble protein was performed according to the method of Laemmli
174 (1970), using polyacrylamide gels (10% Mini-PROTEAN® TGX™ Precast Protein Gels, 12-well, 20
175 µL) from Bio-Rad (Bio-Rad Laboratories, S.A., Madrid, Spain). The electrode buffer (pH 8.3)
176 contained 0.25 M TRIS-HCL, 1.92 M glycine and 1% sodium dodecyl sulfate (SDS). The samples
177 were mixed in a proportion of 1:1 with the loading buffer, which contained 50 mM TRIS-HCL
178 (pH 6.8), 10% β-mercaptoethanol, 2 mM EDTA, 0.1% bromophenol blue, 5% SDS and 30%
179 glycerol. The final concentration of the protein was 2–3 mg/mL. Samples were heated at 90 °C
180 for 5 min and loaded (15 µl) into the gel until the marker reached the bottom of the gel. A
181 molecular weight standard (Precision Plus Protein™ All Blue Prestained Protein Standards)
182 from Bio-Rad was also loaded (10 µl). Protein bands were stained in a solution containing 0.1%
183 Coomassie blue, 50% methanol and 10% acetic acid, under continuous agitation for 1 h.
184 Destaining was performed in an aqueous solution of 30% methanol and 10% acetic acid. The
185 gel was conserved in a solution of 5% glycerol and 10% acetic acid.

186 **2.5.3. Particle size and zeta potential of soluble protein aggregates**

187 Particle size (% in intensity) and zeta potential measurements of salt-ground muscle soluble
188 protein were performed by dynamic light scattering using the Zetasizer Nano ZS (Malvern
189 Instruments Ltd., Worcestershire, UK) at ≤5 °C. The samples were also diluted with 0.2 M
190 phosphate buffer (pH 7) at a final concentration of 0.01 mg/mL and 10 replicates per sample
191 were measured.

192 **2.5.4. Differential scanning calorimetry (DSC)**

193 DSC analysis was performed using a model TA-Q1000 Differential Scanning Calorimeter (TA
194 Instruments, New Castle, DE, USA) previously calibrated by running high purity indium (melting
195 point, 156.4 °C; melting enthalpy, 28.44 J/g). Salt-ground muscle samples (≈10–12 mg) were
196 tightly encapsulated in aluminium hermetic pans. An empty pan was used as reference. They
197 were scanned under dry nitrogen purge (50 mL/min) from 2 °C to 90 °C, at a heating rate of 10

°C/min. After cooling down to 2 °C at 10 °C/min, a second scan in the same conditions was run to check for reversible effects. Endothermic peak temperature (T peak, °C) and transition enthalpy (ΔH, J/g) were calculated by sigmoidal baseline integration using the TA Instrument Universal Analysis 2000 software. At least three replicates were measured per sample.

2.5.5. Relaxometry analysis

Relaxometry analysis was carried out according to Sánchez-Alonso, Moreno & Careche (2014), using a Low-Field Nuclear Magnetic Resonance (LF-NMR) Minispec mq20 analyser (Bruker Optik GmbH, Germany) with a magnetic field strength of 0.47 T (proton resonance frequency of 20 MHz). A weighted amount of ≈2 g salt-ground muscle (1x1x2 cm) was placed in NMR tubes (1.8 cm diameter and 18 cm height). Sample temperature was kept at 4 °C using a Thermo Haake® C/DC class DC10-K10 refrigerated circulator (Fisher Scientific S.L., Madrid, Spain). Transverse relaxation data (T_2) were measured using the Carr–Purcell Meiboom–Gill pulse sequence with a τ-value of 150 μs, and 16 scans at 2 s intervals with a total of 3000 echoes were obtained per sample. Relaxation time distribution was analysed using the CONTIN regularization algorithm. At least four replicates were measured per sample.

2.5.6. Dynamic oscillatory study

Viscoelastic properties of salt-ground muscle systems (elastic modulus G', viscous modulus G'' and phase angle δ) were determined using a Bohlin rheometer (Bohlin Instruments Ltd., model CVO, Worcestershire, UK) with a cone-plate geometry (cone angle 4°, gap = 0.15 mm). A dynamic frequency sweep was done at 10 °C by applying oscillation amplitude within the linear region (=0.005) over the frequency range 0.1–10 Hz. The dynamic temperature sweep was done by heating from 15 °C to 80 °C at a scan rate of 1 °C/min, frequency of 1 Hz and target strain =0.005. Results were the mean of at least 2 determinations.

2.6. Gel strength

A puncture test was performed on heat-induced gels at 60 °C and 80 °C, using a TA-XT plus Texture Analyser (Texture Technologies Corp., Scarsdale, NY, USA) employing a cylindrical stainless steel plunger (5 mm diameter) attached to a 5 kg load cell, at a speed of 0.33 mm/s and 90% strain. The breaking force (expressed in N) and breaking deformation (expressed in mm) were determined. The gel strength (N·mm) was the product of multiplying the breaking force by the breaking deformation. Results were the mean of three determinations.

2.7. Statistical analysis

Analysis of variance was performed using the SPSS® computer program (IBM SPSS Statistics 22 Software, Inc., Chicago, IL, USA). Differences between means were assessed on the basis of confidence intervals using the Tukey test, with a significance level set at $p \leq 0.05$.

3. Results and Discussion

3.1. Liposome properties

Table 1 presents the results of mean particle size (expressed as z-average), polydispersity index (PDI) and membrane surface charge (zeta potential) of the various liposome dispersions. The dried liposomal preparations were rehydrated in order to acquire again the vesicle intrinsic shape. The HP treatment did not modify any characteristic of the liposomes analysed ($p>0.05$) as compared to the control fresh sample, both preparations (HP and L) showing z-average and zeta potential values of 141 nm and –45 mV, respectively. Furthermore, both samples kept the same essential monomodal particle size distribution, as depicted in Figure 1, and very similar PDI (≈0.23). This finding indicates that soy phosphatidylcholine liposomes could be stabilized from a microbiological point of view at a pressure as high as 600 MPa for 20 min without suffering particle fusion or aggregation phenomena. However, slight structural changes in the vesicle membrane cannot be discounted. In this respect, pressure-induced morphological

246 changes as well as interdigitation and changes in bilayer membrane fluidity have been
247 reported when working at lower pressure levels (Braganza & Worcester, 1986; Perrier-Cornet
248 & Gervais, 2005).

249 Conventional freezing at –20 °C and subsequent thawing (FT liposomes) induced a
250 considerable increase in both mean particle size and PDI, and a slight ($p \leq 0.05$) reduction of
251 zeta potential, which denoted partial loss of liposomal stability. This preparation showed a
252 typical bimodal particle size distribution (Figure 1) arising from strong vesicle aggregation, with
253 the main contribution of particles peaking at around 1 μm and a much smaller proportion of
254 particles keeping the original size around 140 nm. The incorporation of glycerol in this
255 liposome formulation (FT-G) significantly ($p \leq 0.05$) reduced the freeze-thawing-induced
256 increase in both particle size (from 507 to 123 nm) and PDI (from 0.545 to 0.220), maintaining
257 the zeta potential value without a significant difference ($p > 0.05$) with respect to the fresh
258 liposomal dispersion (L). The monomodal size distribution profile of FT-G shifted towards lower
259 values even as compared to the control L liposomes (Figure 1). Cryoprotectants, including
260 glycerol, have been widely utilized in the preparation of liposomes. According to Mozafari
261 (2005), this compound improves vesicle stability, avoiding particle aggregation and
262 sedimentation in freezing and thawing processes, and may also prevent structural damage
263 upon lyophilization. The increase in the viscosity of the phospholipid liposome system
264 formulated with glycerol has also recently been associated with higher stability (Vitonyte et al.,
265 2017). In the case of freeze-dried and rehydrated liposomes (FD), the particle size and PDI also
266 exhibited a significant increase ($p \leq 0.05$) with respect to the fresh sample (L), but the alteration
267 was much smaller than in the freeze-thawed (FT) preparations, and in fact no particle
268 destabilization was observed (no significant change in zeta potential value). For freeze-drying,
269 the freezing temperature used was noticeably lower than for conventional freezing treatment
270 (–80 °C vs. –20 °C), but the water removal probably led to breaking of hydrogen bonds
271 between water molecules and phospholipid head groups, leading to some liposome

aggregation (Stark et al., 2010; Chen et al., 2010). In freeze-dried liposomal preparations, the addition of glycerol (FD-G) noticeably increased the mean particle size without a significant change in the PDI, both samples (FD and FD-G) showing monomodal particle size distribution (Figure 1). The FD-G liposomal dispersion had the highest ($p \leq 0.05$) zeta potential, denoting very good particle stability. The addition of glycerol for liposome production interfered with the structure and modified the fluidity of the membrane bilayer, leading to a slight increase in particle size (Manca et al., 2013; Taladrid et al., 2017). The amount and type of cryoprotectant, the preparation process, lyophilization conditions and lipid composition are important factors determining the final vesicle size (Arshinova, Sanarova, Lantsova & Oborotova, 2012).

The spray-dried liposomal preparation (SD) did not differ significantly ($p > 0.05$) from the freeze-dried sample (FD) in relation to mean particle size (z-average), PDI or zeta potential (Table 1). This result supports the idea that the slight change in vesicle characteristics observed in the FD sample with respect to the freshly prepared liposome dispersion was more the result of drying than of the freezing process, which took place at –80 °C. A similar effect was previously reported when comparing fresh and atomized liposomes (Frenzel, Krolak, Wagner & Steffen-Heins, 2015). The smaller particle size of the SD liposomes (178 nm) in the present work compared with others reported in the literature (around 400–430 nm) (Frenzel et al., 2015; Wang et al., 2015) could be mainly attributed to the drying conditions, as well as to the type or the initial size of the liposomes. Telang and Thorat (2010) demonstrated that variations in atomization conditions (inlet and outlet temperatures, aspiration rate, feed flow rate, air flow rate and pressure) had a strong influence on particle size after rehydration, as well as on other properties such as moisture content, porosity, cohesiveness, dispensability, etc.

The freeze-dried liposomal preparation (FD) had the appearance of a fine powder. In contrast, the FD-G sample presented a pasty and somewhat gluey consistency, attributed to the high density and plasticizing effect of glycerol. The presence of glycerol yielded a dried product (FD-

297 G) with considerably higher moisture, attributed mainly to the highly hygroscopic nature of
298 glycerol. Freeze-drying resulted in more effective water removal as compared to spray-drying,
299 with residual moisture contents of 4.8% and 19% in FD and SD samples, respectively (Table 1).
300 In fact, the SD liposomal preparation had the consistency of a paste rather than a dry powder.
301 The relatively high final moisture content in the SD sample could be due to the high aspiration
302 rate employed (70%), which could partially hamper water extraction (Telang & Thorat, 2010).
303 All the preparations studied showed very high dispersibility in water (higher than 99%),
304 including the freeze-dried and spray-dried samples (Table 1). The value was significantly
305 reduced in the glycerol-containing samples, especially in FD-G, with 71.3% dispersibility.
306 Glycerol has proved to be suitable for preserving liposomes from freeze-induced vesicle
307 aggregation, with minimal changes in physical properties and water solubility; however, its
308 effectiveness for preventing dehydration-induced vesicle damage is more limited. In this
309 respect, disaccharides such as sucrose or trehalose were reported to be more effective
310 lyoprotectants (Stark et al., 2010).

311 **3.2. Characterization of salt-ground muscle systems**

312 **3.2.1. Moisture, water holding capacity and soluble protein**

313 The moisture content, soluble protein and water holding capacity (WHC) of the salt-ground
314 muscle without and with added liposomes are shown in Table 2. The final moisture in the
315 samples studied ranged from 84.0 to 86.9%, which was noticeably higher than the raw muscle
316 water content (80 ± 1.5%). A considerable amount of water was incorporated in the final
317 muscle formulation either by direct addition of the aqueous liposome dispersions (L, HP, FT
318 and FT-G liposomes) or by adding the amount of water calculated as being necessary to adjust
319 the moisture content of the muscle systems without (control) or with the dried preparations
320 (FD, FD-G and SD). All liposome-containing samples presented very close moisture levels (84–
321 85%), slightly lower than in the control sample without liposomes (86.9%). This slight

322 difference was probably due to the dry matter content of the liposomal dispersions, since it
323 was replaced by the same volume of water in the control sample.

324 The soluble protein was highest in the control salt-ground muscle (M system). All the
325 liposome-containing systems presented soluble protein values close to 70%, with the
326 exception of those containing the freeze-dried preparations, which had values of 63% (FD-G)
327 and 56% (FD). The pasty consistency and lower water dispersibility of the freeze-dried
328 liposomal preparation with glycerol (see Table 1) were apparently not crucial factors for the
329 reduced myofibrillar protein solubility, since it was significantly lower ($p \leq 0.05$) in the FD
330 preparation, which was a highly water dispersible powder. Both FD and FD-G samples did not
331 show any distinctive vesicle properties (particle size or zeta potential), and the most striking
332 feature was the lower water content of the liposomal preparation, which was <15% in FD-G
333 and <5% in FD samples (Table 1). They may have established competition with the myofibrillar
334 protein for the water molecules, causing protein dehydration and aggregation which could not
335 be countered with the amount of water added for moisture adjustment. This effect was not
336 seen in the atomized liposomes, possibly because the residual water content in the SD
337 preparation was slightly higher. These results might indicate that the presence of liposomes in
338 the salt-ground muscle induced aggregation of the myofibrillar protein, or that they interfered
339 with the salt-induced protein unfolding during muscle grinding.

340 The water holding capacity (WHC) was considerably higher ($p \leq 0.05$) in the liposome-containing
341 samples than in the control batch. No clear relationship could be established between WHC
342 and protein solubility in the samples studied, but the WHC values were inversely correlated
343 with the moisture content ($r = -0.81$). In the control batch, which presented the highest
344 moisture, probably too much water was added, so the unfolded protein was not able to retain
345 it properly. In contrast, in the liposome-containing batches water molecules could be
346 efficiently bound to the polar head groups at the liposome membrane surface, which could

increase the overall hydration state of the surrounding myofibrillar protein. This effect was less pronounced with the dried liposomal preparations. The addition of glycerol to the liposome formulation slightly reduced ($p \leq 0.05$) the moisture content in the corresponding salt-ground muscles (FT-G vs. FT and FD-G vs. D), with a concomitant increase in WHC. In general, liposome size or surface membrane charge did not have a significant effect on muscle WHC or protein solubility. However, the low moisture content in dehydrated liposomal preparations seems to be a more important feature in reducing both WHC and soluble protein content, probably by competing with protein chains for water molecules. Among all the batches with liposomes, the one containing the lyophilized product (FD) presented the lowest values of both WHC and protein solubility.

3.2.2. SDS-PAGE of soluble protein

The soluble protein electrophoretic profile of the various muscle systems with or without liposomes is shown in Figure 2. All batches presented the same molecular weight pattern, which was characterized by the predominance of an intense band at ≈200 kDa tentatively assigned to the myosin heavy chain (MHC), as well as other prominent bands of molecular weight below 50 kDa, which could be associated with the presence of other main myofibrillar protein components, namely actin, troponins, tropomyosin and myosin light chains (Paredi, Pagano & Crupkin, 2010). A certain amount of high molecular weight protein aggregates that could not enter the stacking gel was observable in all batches, including the control muscle system (M). These results indicated that, regardless of the type of liposome added, the myofibrillar proteins were solubilized in a similar way from a qualitative point of view. A lower-intensity MHC band would have indicated significant crosslinking, causing this protein to remain in the insoluble protein fraction. Thus, no evident signs of covalent protein-lipid interactions taking part of the soluble protein aggregates were observed. The lower protein solubility found in the liposome-containing batches could be mostly attributed to non-covalent

372 interactions, probably hydrogen bonding between protein side chains and liposome
373 membrane polar head groups or attached water molecules.

374 **3.2.3. Zeta potential and particle size of soluble protein**

375 The soluble protein of the control salt-ground muscle (M) showed electronegative zeta
376 potential (Table 3). The negative protein charge at the neutral muscle pH could be the result of
377 deprotonation of acidic amino acids, such as glutamic acid and aspartic acid, which are
378 abundant in fish muscle. The negative protein charge in the present work is slightly higher than
379 that reported in heated natural actomyosin solutions from sardine muscle (Vate & Benjakul,
380 2016). Despite the strong electronegative zeta potential of liposomes, their addition to the
381 muscle system did not induce significant changes ($p>0.05$) in the protein surface charge,
382 except in the case of the FT batch, which presented a slight increase. These results indicate
383 minimal protein conformational changes induced by electrostatic repulsions among negative
384 charges of both protein carboxyl and phosphate liposomal groups.

385 DLS was used to gain an insight into the particle size distribution of the salt-soluble protein
386 aggregates in the various muscle systems (Figure 3), which could not be evidenced by the
387 electrophoretic study. The soluble protein fraction of the control system without liposomes
388 (M) showed a bimodal particle size distribution, with the predominance of a protein aggregate
389 population peaking at ≈825 nm, which would correspond to the bulk of the denatured salt-
390 soluble proteins. Another low contribution of smaller protein fragments was found to peak at
391 around 164 nm, coinciding with the length of the entire myosin molecule (Lanier,
392 Yongsawatdigul & Carvajal-Rondanelli, 2013). The addition of liposomes in the form of
393 aqueous dispersions (Figure 3a) induced less noticeable changes in the size distribution of
394 protein aggregates than when added in the dried form (Figure 3b). In the case of the HP batch,
395 both peaks showed reduced intensity and shifted to a lower particle size, with a concomitant
396 appearance of a small peak at ≈5.5 µm. This behaviour seems to indicate disintegration of big

sized protein aggregates into smaller ones, with concomitant appearance of new bigger aggregates in lower amount. Despite having the same hydrodynamic particle properties, the HP liposomal dispersion induced more protein conformational disturbance than the fresh liposomes. Although it could not be visualized, HP processing could have promoted more hydrogen-bound water molecules attached to the liposome membrane surface, which would affect protein-protein interactions to a greater extent than the fresh liposomes. When liposomes were added in the dried state, the signal corresponding to the main protein aggregates at ≈825 nm was considerably lower, with smaller and more dispersed-size aggregates. In parallel, big aggregates of ≈5.5 μm were observed, more markedly with the atomized (SD) sample. In agreement with the lower protein solubility, these findings suggest that liposomes added in the dry state might hinder adequate protein denaturation and solubilization during the muscle salt-grinding step.

3.2.4. Differential scanning calorimetry (DSC)

The thermal properties of the various salt-ground muscle systems are shown in Table 3 and Figure 4. The DSC thermogram of the control system (M) was characterized by two main endothermic events (onset T_0) occurring at 40.5 °C and 61.2 °C, associated with thermal denaturation of the myosin rod (first event) and F-actin (second event), respectively. According to Careche, del Mazo & Fernandez-Martín (2002), the first event actually might correspond to myosin composite with connective tissue protein. Another minor thermal transition, hardly visible at a T_0 of 27.8 °C, was assigned to the myosin subfragment S1. The main transitions appeared somewhat diffuse in the DSC trace and shifted to a slightly lower temperature than that reported for both myosin and actin in fresh whole hake muscle (Beas, Wagner, Crupkin & Añón, 1990; Careche et al., 2002). This effect, which was much more noticeable in the case of the myosin rod, was the result of muscle homogenization and salt-blending, causing protein destabilization and unfolding (Fernández-Martín, Pérez-Mateos & Montero, 1998). F-actin

appeared to be much more resistant to salt-induced denaturation than myosin, as deduced from the more pronounced endothermic event. The addition of liposomes to the salt-ground muscle caused a significant increase ($p \leq 0.05$) in the three main transition temperatures, indicating increased thermal stability of both myosin and actin. The type of liposomal preparation did not appear to produce any great differential change in denatured myosin thermal behaviour. In contrast, the increase in thermal stability of F-actin as a result of liposome addition was higher when liposomes were added in the dry state (FD, FD-G and SD). These batches were characterized by higher liposomal interference in the size distribution of protein aggregates, as mentioned above, with the appearance of bigger sizes, probably resulting from insufficient protein solubilization. The lower enthalpy produced by the addition of liposomes indicated a noticeable conformational change in the actin filaments, probably because they were originally less affected by salt than the myosin rod.

3.2.5. LF-NMR-^{1}H analysis

Figure 5 shows the transversal proton relaxation time curves in the various salt-ground muscle systems, in order to evaluate differences in chemical proton exchange (essentially water) that might be associated with protein morphological changes, denaturation and aggregation (Erikson, Standal, Aursand, Veliyulin & Aursand, 2012). The main relaxation component (T_{2a}), which represents water located within highly organized protein structures, peaked in the range of 77.8–92.5 ms. Considerably shorter relaxation times were reported for the T_{2a} water population, referred to as T_{21} in either frozen or unfrozen hake muscle (Sánchez-Alonso et al., 2014). This difference could be attributed to an increased relaxation time of water in the intramyofibrillar space owing to the salt-induced protein unfolding, which caused the protein network to expand. A slower relaxation component ($T_{2a'}$ at 273.3 ms) was clearly visible in the control muscle system without liposomes. This population corresponds to extra-myofibrillar water that could be lost as drip. This $T_{2a'}$ component was reported to appear in hake muscle as

447 an extra band in the range of 120–360 ms, resulting from morphological protein changes after
448 freezing (Sanchez-Alonso et al., 2014). This relaxation behaviour in the salt-ground muscle
449 indicates chemical exchange between water and protein protons resulting from salt-induced
450 protein denaturation (Hills, Wright & Belton, 1989). The addition of the liposomal preparations
451 led to noticeable increases in both T_{2a} relaxation time and amplitude, strongly suggesting an
452 increase in the spacing between the myofibrils, leading to more water being trapped within
453 the myofibrillar protein network. The liposome-containing muscle systems did not present any
454 significant proton exchange event at the $T_{2a'}$ relaxation time, indicating that the amount of
455 water located outside the myofibrillar protein network was negligible. Furthermore, a fast
456 minor component (T_{2b}) that took place at a relaxation time of 1.1–1.3 ms in the systems with
457 liposomes was hardly visible in the control system. This proton relaxation component is related
458 to the presence of water tightly associated with macromolecules (Erikson et al., 2012).

459 These findings were consistent with the noticeable increase in water holding capacity resulting
460 from addition of liposomes to the salt-ground muscle. Among the various types of liposomes
461 added, the fresh (L) and pressurized (HP) liposome dispersions led to higher ($p \leq 0.05$)
462 amplitudes in the T_{2a} relaxation component than any other preparation. This finding, however,
463 could not be related to significant differences in moisture, WHC or protein solubility of the
464 corresponding muscle systems. However, the higher T_{2a} amplitude in the HP batch would be in
465 agreement with a higher amount of attached water molecules at the liposome membrane
466 surface, causing stronger protein conformational disturbance.

467 **3.2.6. Dynamic oscillatory rheology**

468 The degree of salt-induced protein denaturation or aggregation in the presence or absence of
469 liposomes was also assessed by determining the viscoelastic behaviour of the corresponding
470 muscle systems, as a function of the oscillation frequency at 10 °C. In all salt-ground muscles,
471 G' prevailed over G" throughout the frequency range studied, indicating a viscoelastic gel-like

behaviour (Badii & Howell, 2002). The results of the elastic modulus and viscous modulus determined at 1 Hz (G'_{1Hz} and G''_{1Hz}, respectively), are presented in Table 3. Differences in both G' and G'' values were, in general, low among the various batches. The addition of the aqueous liposome dispersions tended to decrease the gel-like consistency, especially in FT liposomes. In contrast, both freeze-dried preparations (FD and FD-G) caused a slight increase ($p \leq 0.05$) in the viscoelastic parameters. All mechanical spectra fitted the power law model, with $R^2 > 0.99$ for G' and $R^2 \geq 0.85$ for G'' values. The power law exponent n' is related to structural stability and protein network conformation: the higher the n' values, the higher the instability of the matrix against frequency changes (Ojagh, Núñez-Flores, López-Caballero, Montero & Gómez-Guillén, 2011). As shown in Table 3, the increase in n' indicates that liposomes might be producing higher matrix discontinuity by interfering with protein-protein interactions. This effect was more pronounced when liposomes were added in the form of an aqueous dispersion, probably because they could access the protein side chains more easily. This finding would agree with the increased intramyofibrillar space with more trapped water inside.

Figure 6 shows the changes in the elastic modulus (G') and phase angle (δ) of the various muscle systems as a function of heating temperature (from 15 °C to 80 °C). The temperature sweep test revealed noticeable differences in protein thermal aggregation profile, depending on the type of liposomal preparation added. Upon heating the control salt-ground muscle from 20 °C upwards, protein destabilization firstly occurred owing to the breakdown of heat-labile hydrogen bonds. This effect promoted protein unfolding, causing greater exposure of reactive sites, which was necessary to form subsequent intermolecular bonds. The relative G' peak observed at 37 °C in the M batch is associated with the so-called setting phenomenon, and corresponded to the formation of a preliminary ordered protein network stabilized by relatively strong protein-protein interactions. Interactions at this temperature range are preferentially hydrophobic interactions and ε-(γ-glutamyl)-lysine covalent bonds induced by endogenous transglutaminase activity (Lanier et al., 2013). The subsequent drop in G' peaking

498 at 47 °C is a typical *modori* phenomenon, which could be the result of protein network
499 disintegration due to optimum activity of heat-stable proteases. The progressive rise in G'
500 values and coincident decline in phase angle as the temperature rose from ≈48 °C to 80 °C
501 indicated the formation of a thermostable gel protein network, which was strengthened
502 predominantly by hydrophobic interactions as well as by intra- and intermolecular
503 thermostable disulfide covalent bonds. The addition of aqueous liposome dispersions
504 increased the G' values considerably in the setting temperature range and thereafter. In fact,
505 the temperature at which maximum G' was achieved shifted to lower values in all these
506 batches (≈60 °C), indicating that liposome dispersions led to much faster protein gelation.
507 Furthermore, weaker gels were obtained, as deduced from the higher phase angle values at
508 the maximum gelling point. A possible explanation could be that the higher matrix
509 discontinuity resulting from increased intramyofibrillar spacing would promote more exposure
510 of protein reactive sites at the onset of heating, leading to a considerable subsequent increase
511 in heat-induced hydrophobic interactions and later also stronger disulfide bonds. The fast and
512 excessive protein interactions would presumably lead to a less ordered gel protein network. It
513 should be noted that apparently the presence of liposomes did not hinder the result of the
514 endogenous TGase activity (setting) or the subsequent autolytic protein degradation (*modori*).
515 When liposomes were added in the dried form, the thermal aggregation profile resembled that
516 of the control system, but differing essentially in that from ≈55 °C onwards the increase in G'
517 was much more limited. The higher phase angle up to the end of heating indicated that the
518 gels produced were also weaker. This behaviour would support the hypothesis that the
519 addition of dry liposomal preparations during the muscle grinding step might hinder protein
520 solubilization and unfolding, so a lower amount of protein reactive sites would be available for
521 subsequent protein thermal gelation.

522 **3.2.7. Mechanical properties**

Puncture force (N), deformation (mm) and gel strength (N·mm) of the gels heated at 60 °C and 80 °C are shown in Figure 7. The control gel (M) presented the highest ($p \leq 0.05$) gel strength values at both temperatures studied. The higher gel strength in the control system was due to higher puncture force, since no significant differences were found among the various batches regarding breaking deformation. Cardoso, Mendes, Saraiva, Vaz-Pires and Nunes (2010) reported higher gel strength for hake mince gels heated at 90 °C for 1 h, which could be partly due to their lower moisture content. The decrease in gel strength as a result of liposome addition has previously been reported in squid surimi gels (Marín et al., 2018). The gels with wet liposomes presented higher puncture force than gels with dried preparations, with the sole exception of the HP batch. Although the gel strength of all the gels at 80 °C followed the same pattern as the gels at 60 °C, their values were higher owing to the increase in both force and deformation. This was presumably because the gels continued to form from 60 to 80 °C for all the formulations, regardless of the type of liposomes added. The apparent inconsistency with respect to the dynamic oscillatory study, in which the batches containing the wet liposomes presented the maximum gelling point at 60 °C, could be caused by the different heating regime. These results confirm that the presence of liposomes interfered strongly with the thermal aggregation of muscle proteins, although the mechanisms for this interference seem to be different depending on the type of liposomal preparation.

4. Conclusions

Technological stabilization treatments induced noticeable changes in liposome properties, with freezing being the method that increased the particle size the most. The key factor influencing muscle protein interactions and thermal gelation was the liposome hydration state rather than the particle size or surface membrane charge. In general, the addition of liposomal preparations to the salt-ground muscle contributed to an increase in the water binding of the system and interfered in the protein thermal gelation. Liposomes in the wet form (aqueous

548 dispersions) induced a fast gelation by favouring protein unfolding during muscle salt-grinding,
549 in contrast to liposomal preparations added in the dry state, which might hinder adequate salt-
550 induced protein solubilisation. Despite the slight reduction in gel strength, the hake muscle
551 added with liposomes constitutes a reliable matrix for developing gel-like fish products with
552 high nutritional and healthy potential. At the same time, this approach will be also useful to
553 valorise hake from eventual discards.

554

555 **Acknowledgements**

556 The authors wish to thank the Spanish Ministry of Economy and Competitiveness (MINECO) for
557 financial support (project AGL2014-52825 and AGL2017-84161-C2-1-R). We are grateful to the
558 Analysis Service Unit of ICTAN-CSIC for the DSC analysis.

559 **References**

560 1. A.O.A.C. (2005). Official methods of analysis. Gaithersburg, MD, USA: Association of Official
561 Analytical Chemists.

562 2. Arshinova, O.Y., Sanarova, E.V., Lantsova, A.V. & Oborotova, N.A. (2012). Drug synthesis
563 methods and manufacturing technology. *Pharmaceutical Chemistry Journal, 46 (4)*, 228-233.

564 3. Badii, F., & Howell, N.K. (2002). Effect of antioxidants, citrate, and cryoprotectants on
565 protein denaturation and texture of frozen cod (Gadus morhua). *Journal of Agricultural and*
566 *Food Chemistry, 50(7)*, 2053-2061.

567 4. Beas, V.E., Wagner, J.R., Crupkin, M., & Ańon, M.C. (1990). Thermal Denaturation of Hake
568 (Merluccius hubbsi) Myofibrillar Proteins. A Differential Scanning Calorimetric and
569 Electrophoretic Study. *Journal of Food Science, 55 (3),* 683-687.

570 5. Braganza, L.F.; & Worcester, D.L. 1986. Hydrostatic pressure induces hydrocarbon chain
571 interdigitation in single component phospholipid bilayer. *Biochemistry, 25*, 2591-2596.

572 6. Cardoso, C.L., Mendes, R.O., Saraiva, J.A., Vaz-Pires, P.R. &Nunes, M.L. (2010). Quality
573 characteristics of high pressure-induced hake (Merluccius capensis) protein gels with and
574 without MGTase. *Journal of Aquatic Food Product Technology, 19*, 193-213.

575 7. Cardoso, C., Mendes, R., Pedro, S., & Nunes, M.L. (2008). Quality changes during storage of
576 fish sausages containing dietary fiber. *Journal of Aquatic Food Product Technology, 17 (1),* 73-
577 95.

578 8. Careche, M., Mazo, ML. & Fernández-Martín, F. 2002. Extractability and thermal stability of
579 frozen hake (*Merluccius merluccius*) fillets stored at -10 and -30°C. *Journal of the Science of*
580 *Food and Agriculture*, 82, 1791–1799.

581
582 9. Chen, C., Han, D., Cai, C., & Tang, X. (2010). An overview of liposome lyophilization and its
583 future potential. *Journal of Controlled Release, 142*, 299–311.

584 10. da Silva Malheiros, P., Daroit, D.J., & Brandelli, A. (2010). Food applications of liposome-
585 encapsulated antimicrobial peptides. *Trends in Food Science and Technology, 21 (6),* 284-292.

586 11. Erikson, U., Standal, I.B., Aursand, I.G., Veliyulin, E. & Aursand, M. (2012). Use of NMR in
587 fish processing optimization: a review of recent progress. *Magnetic Resonance in Chemistry,*
588 *50*, 471-480.

589 12. Fernández-Martín, F., Pérez-Mates, M., & Montero, P. 1998. Effect of pressure/heat
590 combinations on blue whiting (*Micromesistius poutassou*) washed mince: thermal and
591 mechanical properties. *Journal of Agricultural and Food Chemistry, 46*, 3257-3264.

592 13. Frenzel, M., Krolak, E., Wagner, A.E. & Steffen-Heins, A. (2015). Physicochemical properties
593 of WPI coated liposomes serving as stable transporters in a real food matrix. *LWT-Food Science*
594 *and Technology, 63,* 527-534.

595 14. Gómez-Guillén, M.C., Montero, P., Hurtado, O., & Borderías, A.J. 2000. Biological
596 characteristics affect the quality of farmed Atlantic salmon and smoked muscle. *Journal of*
597 *Food Science, 65,* 53-60

598 15. Gültekin-Özgüven, M., Karadağ, A., Duman, S., Özkal, B. &Özçelik, B. (2016). Fortification of
599 dark chocolate with spray dried black mulberry (Morus nigra) waste extract encapsulated in
600 chitosan-coated liposomes and bioaccessability studies. *Food Chemistry, 201*, 205-212.

601 16. Hills, B.P., Wright, K.M., & Belton, P.S. (1989). N.M.R. studies of water proton relaxation in
602 Sephadex bead suspensions. *Molecular Physics, 67(1*), 193–208.

603 17. Laemmli, U.K. (1970). Cleavage of structural proteins during the assembly of the head of
604 bacteriophage T4. *Nature, 227 (5259*), 680-685.

605 18. Lanier, T.C., Yongsawatdigul, J., & Carvajal-Rondanelli, P. (2013). Surimi Gelation Chemistry.
606 In J.W. Park (Ed.), *Surimi and Surimi Seafood* (pp. 101–140). CRC Press. Taylor & Francis Group.

607 19. Laye, C., McClements, D.J., & Weiss, J. (2008). Formation of biopolymer-coated liposomes
608 by electrostatic deposition of chitosan. *Journal of Food Science, 73 (5),* N7–N15.

609 20. Manca, M.L., Zaru, M., Manconi, M., Lai, F., Valenti, D., Sinico, C., & Fadda, A.M. (2013).
610 Glycerosomes: A new tool for effective dermal and transdermal drug delivery. *International*
611 *Journal of Pharmaceutics, 455,* 66–74.

612 21. Marín, D., Alemán, A., Sánchez-Faure, A., Montero, P., & Gómez-Guillén, M.C. (2018).
613 Freeze-dried phosphatidylcholine liposomes encapsulating various antioxidant extracts from
614 natural waste as functional ingredients in surimi gels. *Food Chemistry, 245*, 525-535.

615 22. Martelo-Vidal, M.J., Guerra-Rodríguez, E., Pita-Calvo, C., & Vázquez, M. (2016). Reduced-
616 salt restructured European hake (Merluccius merluccius) obtained using microbial
617 transglutaminase. *Innovative Food Science and Emerging Technologies, 38*, 182-188.

618 23. Moreno, H.M., Javier Borderías, A., & Baron, C.P. (2010). Evaluation of some physico-
619 chemical properties of restructured trout and hake mince during cold gelation and chilled
620 storage. *Food Chemistry, 120,* 410-417.

621 24. Mozafari, M. R. (2005). Liposomes: An overview of manufacturing techniques. *Cellular and*
622 *Molecular Biology Letters, 10(4)*, 711-719.

623 25. Mozafari, M.R., Johnson, C., Hatziantoniou, S., & Demetzos, C. (2008). Nanoliposomes and
624 their applications in food nanotechnology. *Journal of Liposome Research, 18*, 309–327.

625 26. Ojagh, S.M., Núñez-Flores, R., López-Caballero, M.E., Montero, M.P., & Gómez-Guillén,
626 M.C. (2011). Lessening of high-pressure-induced changes in Atlantic salmon muscle by the
627 combined use of a fish gelatin-lignin film. *Food Chemistry, 125 (2*), 595-606.

628 27. Paredi, M.E., Pagano, M.R., Crupkin, M. (2010). Biochemical and Physicochemical
629 Properties of actomyosin and myofibrils from frozen stored flounder (*Paralichthys*
630 *patagonicus*) fillets. *Journal of Food Biochemistry*, 34 (5), 983-997.

631 28. Perrier-Cornet, J.M., & Gervais, K.B. 2005. Pressure-induced shape change of phospholipid
632 vesicles: implication of compression and phase transition. *Journal of Membrane Biology*, 204,
633 101-107.

634 29. Rigaldie, Y., Largeteau, A., Lemagnen, G., Ibalot, F., Pardon, P., Demazeau, G., & Grislain, L.
635 (2003). Effects of High Hydrostatic Pressure on Several Sensitive Therapeutic Molecules and a
636 Soft Nanodispersed Drug Delivery System. *Pharmaceutical Research, 20 (12*), 2036-2040.

637 30. Sánchez-Alonso, I., Moreno, P., & Careche, M. 2014. Low field nuclear magnetic resonance
638 (LF-NMR) relaxometry in hake (Merluccius merluccius, L.) muscle after different freezing and
639 storage conditions. *Food Chemistry, 153*, 250-257.

640 31. Sebaaly, C., Greige-Gerges, H., Stainmesse, S., Fessi, H. & Charcosset, C. (2016). Effect of
641 composition, hydrogenation of phospholipids and lyophilisation on the characteristics of
642 eugenol-loaded liposomes prepared by the ethanol injection method. *Food Bioscience, 15*, 1-
643 10.

644 32. Stark, B., Pabst, G. & Prassl, R. (2010). Long-term stability of sterically stabilized liposomes
645 by freezing and freeze-drying: Effects of cryoprotectants on structure. *European Journal of*
646 *Pharmaceutical Sciences, 41 (3-4)*, 546–555.

647 33. Taladrid, D., Marín, D., Alemán, A., Álvarez-Acero, I., Montero, P., & Gómez-Guillén, M.C.
648 (2017). Effect of chemical composition and sonication procedure on properties of food-grade
649 soy lecithin liposomes with added glycerol. *Food Research International, 100*, 541-550.

650 34. Telang, A.M. & Thorat, B.N. (2010). Optimization of Process Parameters for Spray Drying of
651 Fermented Soy Milk. *Drying Technology, 28 (12*), 1445-1456.

652 35. Vate, N.K., & Benjakul, S. (2016). Combined effect of squid ink tyrosinase and tannic acid on
653 heat induced aggregation of natural actomyosin from sardine. *Food Hydrocolloids, 56*, 62-70.

654 36. Vitonyte, J., Manca, M.L., Caddeo, C., Valenti, D., Peris, J.E., Usach, I., … Orrù, G. (2017).
655 Bifunctional viscous nanovesicles co-loaded with resveratrol and gallic acid for skin protection
656 against microbial and oxidative injuries. *European Journal of Pharmaceutics and*
657 *Biopharmaceutics, 114,* 278-287.

658 37. Wang, L., Hu, X., Shen, B., Xie, Y., Shen, C., Lu, Y., … Wu, W. (2015). Enhanced stability of
659 liposomes against solidification stress during freeze-drying and spray-drying by coating with
660 calcium alginate. *Journal of Drug Delivery Science and Technology, 30*, 163-170.

661 38. Zhou, L.S., Li-Chan, & E.C.Y. (2009). Effects of Kudoa spores, endogenous protease activity
662 and frozen storage on cooked texture of minced Pacific hake (Merluccius productus). *Food*
663 *Chemistry, 113 (4),* 1076-1082.

664

665
666

667

668 FIGURE CAPTIONS

669 FIGURE 1. Particle size distribution of liposome dispersions: L (Fresh), HP (High Pressure), FT
670 (Freeze-thawed), FT-G (Freeze-thawed with glycerol), FD (Freeze-dried), FD-G (Freeze-dried
671 with glycerol), SD (Spray-dried).

672 FIGURE 2. SDS-PAGE of the soluble protein fraction from salt-ground muscle (M) alone and
673 with added liposomal preparations: L (Fresh), HP (High Pressure), FT (Freeze-thawed), FT-G
674 (Freeze-thawed with glycerol), FD (Freeze-dried), FD-G (Freeze-dried with glycerol), SD (Spray-
675 dried). St. = molecular weight standard.

676 FIGURE 3. Particle size distribution of soluble protein aggregates from salt-ground muscle (M)
677 alone and with added liposomal preparations: L (Fresh), HP (High Pressure), FT (Freeze-
678 thawed), FT-G (Freeze-thawed with glycerol), FD (Freeze-dried), FD-G (Freeze-dried with
679 glycerol), SD (Spray-dried).

680 FIGURE 4. DSC thermograms of salt-ground muscle (M) alone and with added liposomal
681 preparations: L (Fresh), HP (High Pressure), FT (Freeze-thawed), FT-G (Freeze-thawed with
682 glycerol), FD (Freeze-dried), FD-G (Freeze-dried with glycerol), SD (Spray-dried).

683 FIGURE 5. LF-NMR relaxation time distribution of salt-ground muscle (M) alone and with added
684 liposomal preparations: L (Fresh), HP (High Pressure), FT (Freeze-thawed), FT-G (Freeze-
685 thawed with glycerol), FD (Freeze-dried), FD-G (Freeze-dried with glycerol), SD (Spray-dried).

686 FIGURE 6. Temperature sweep test in terms of G' and phase angle (δ) of salt-ground muscle
687 (M) alone and with added liposomal preparations: L (Fresh), HP (High Pressure), FT (Freeze-
688 thawed), FT-G (Freeze-thawed with glycerol), FD (Freeze-dried), FD-G (Freeze-dried with
689 glycerol), SD (Spray-dried).

690 FIGURE 7.- Mechanical properties of gels produced at 60 and 80 °C from salt-ground muscle
691 (M) alone and with added liposomal preparations: L (Fresh), HP (High Pressure), FT (Freeze-
692 thawed), FT-G (Freeze-thawed with glycerol), FD (Freeze-dried), FD-G (Freeze-dried with
693 glycerol), SD (Spray-dried). a) puncture force, b) puncture deformation, c) gel strength.

694

695

696

697 **TABLE 1**. Z-average, polydispersity, ζ-potential, moisture and dispersibility of liposomal
698 preparations: L (Fresh), HP (High Pressure), FT (Freeze-thawed), FT-G (Freeze-thawed with
699 glycerol), FD (Freeze-dried), FD-G (Freeze-dried with glycerol), SD (Spray-dried).

	Z-average (nm)	Polydispersity (PDI)	ζ-Potential (mV)	Moisture (%)	Dispersibility (%)
L	141.3 ± 1.9^{B}	0.225 ± 0.003^{A}	-44.8 ± 1.8^{B}	$93,03 \pm 0.01^{D}$	> 99
HP	141.4 ± 1.2^{B}	0.228 ± 0.008^{A}	-45.0 ± 1.7^{B}	$93,44 \pm 0.38^{D}$	> 99
FT	507.1 ± 12.6^{E}	0.545 ± 0.014^{C}	-39.6 ± 1.2^{C}	$94,04 \pm 0.06^{D}$	> 99
FT-G	123.3 ± 1.0^{A}	0.220 ± 0.011^{A}	-42.9 ± 1.8^{B}	$92,64 \pm 0.20^{D}$	93.40 ± 0.53^{B}
FD	181.0 ± 5.2^{C}	0.332 ± 0.033^{B}	-44.3 ± 1.7^{B}	$4,78 \pm 0.72^{A}$	> 99
FD-G	274.6 ± 5.8^{D}	0.383 ± 0.055^{B}	-49.5 ± 1.0^{A}	$14,87 \pm 2.12^{B}$	71.29 ± 1.81^{A}
SD	177.9 ± 2.8^{C}	0.393 ± 0.025^{B}	-44.6 ± 0.6^{B}	$19,20 \pm 0.84^{C}$	> 99

700 Different letters (A, B, C, D, E) indicate significance differences ($p \leq 0.05$) among samples for each
701 parameter.

702

703

704

705

706 **TABLE 2**. Moisture content, salt-soluble protein and water holding
707 capacity of salt-ground muscle (M) with added liposomal
708 preparations: L (Fresh), HP (High Pressure), FT (Freeze-thawed), FT-
709 G (Freeze-thawed with glycerol), FD (Freeze-dried), FD-G (Freeze-
710 dried with glycerol), SD (Spray-dried).

	Moisture (%)	Salt-Soluble Protein (%)	WHC (%)
M	86.87 ± 0.05^{F}	78.95 ± 0.98^{E}	69.13 ± 4.20^{A}
L	84.59 ± 0.06^{C}	$73.93 \pm 2.52^{C,D}$	$87.17 \pm 2.64^{C,D}$
HP	84.39 ± 0.04^{B}	$68.66 \pm 0.95^{B,C}$	91.37 ± 1.28^{D}
FT	85.60 ± 0.06^{E}	$74.59 \pm 0.96^{C,D}$	$82.10 \pm 3.88^{B,C}$
FT-G	84.07 ± 0.01^{A}	$69.30 \pm 0.73^{B,C}$	92.12 ± 1.75^{D}
FD	84.91 ± 0.03^{D}	55.94 ± 0.27^{A}	76.02 ± 2.02^{B}
FD-G	83.98 ± 0.06^{A}	62.66 ± 0.69^{B}	83.78 ± 2.52^{C}
SD	84.59 ± 0.12^{C}	71.04 ± 4.69^{C}	$81.30 \pm 2.66^{B,C}$

711 Different letters (A, B, C, D, E, F) indicate significance differences
712 ($p \leq 0.05$) among samples for each parameter.

713

714

TABLE 3. Transition temperatures (onset temperature, T_0), enthalpy changes (ΔH), zeta-potential (ζ-potential) and viscoelastic parameters of salt-ground muscle (M) with added liposomal preparations: L (Fresh), HP (High Pressure), FT (Freeze-thawed), FT-G (Freeze-thawed with glycerol), FD (Freeze-dried), FD-G (Freeze-dried with glycerol), SD (Spray-dried).

	$T_0$1 (°C)	$T_0$2 (°C)	$T_0$3 (°C)	ΔH3 (J/g)	ζ-potential (mV)	$G'_{1\ Hz}$ (kPa)	$G''_{1\ Hz}$ (kPa)	n′	n′′
M	27.8 ± 0.7^{a}	40.5 ± 0.9^{a}	61.2 ± 2.4^{a}	0.533 ± 0.075^{a}	-20.8 ± 1.4^{ab}	3.57 ± 0.10^{a}	0.58 ± 0.04^{a}	0.134	0.136
L	32.6 ± 1.9^{b}	42.8 ± 0.1^{bc}	65.4 ± 0.6^{b}	0.254 ± 0.038^{bc}	-19.2 ± 2.2^{b}	3.00 ± 0.05^{b}	0.59 ± 0.01^{ab}	0.161	0.180
HP	29.4 ± 0.1^{cd}	43.9 ± 1.0^{c}	65.7 ± 0.5^{b}	0.186 ± 0.017^{bde}	-21.8 ± 0.4^{ab}	3.35 ± 0.26^{ab}	0.66 ± 0.04^{abc}	0.169	0.171
FT	30.4 ± 1.0^{cef}	44.3 ± 1.9^{c}	65.0 ± 1.3^{b}	0.226 ± 0.048^{bcd}	-28.7 ± 1.1^{c}	2.04 ± 0.07^{c}	0.47 ± 0.00^{d}	0.175	0.219
FT-G	28.7 ± 0.7^{ad}	42.8 ± 0.4^{bc}	65.0 ± 0.1^{b}	0.271 ± 0.037^{c}	-19.5 ± 0.0^{b}	3.16 ± 0.08^{ab}	0.79 ± 0.10^{e}	0.203	0.224
FD	30.0 ± 1.3^{ce}	43.4 ± 2.2^{bc}	67.2 ± 0.2^{c}	0.238 ± 0.010^{bcd}	-24.5 ± 1.3^{a}	4.12 ± 0.36^{d}	0.69 ± 0.04^{bce}	0.149	0.150
FD-G	31.1 ± 0.6^{ef}	42.0 ± 0.5^{b}	67.5 ± 1.1^{c}	0.169 ± 0.017^{de}	-21.2 ± 2.7^{ab}	4.17± 0.34^{d}	0.74 ± 0.07^{ce}	0.156	0.148
SD	31.5 ± 0.6^{bf}	44.3 ± 0.6^{c}	67.6 ± 0.5^{c}	0.126 ± 0.037^{e}	-24.2 ± 1.0^{a}	3.46 ± 0.33^{ab}	0.57 ± 0.05^{d}	0.142	0.126

Different letters (a,b,c…) indicate significance differences ($p \leq 0.05$) among samples for each parameter.

720

721

722

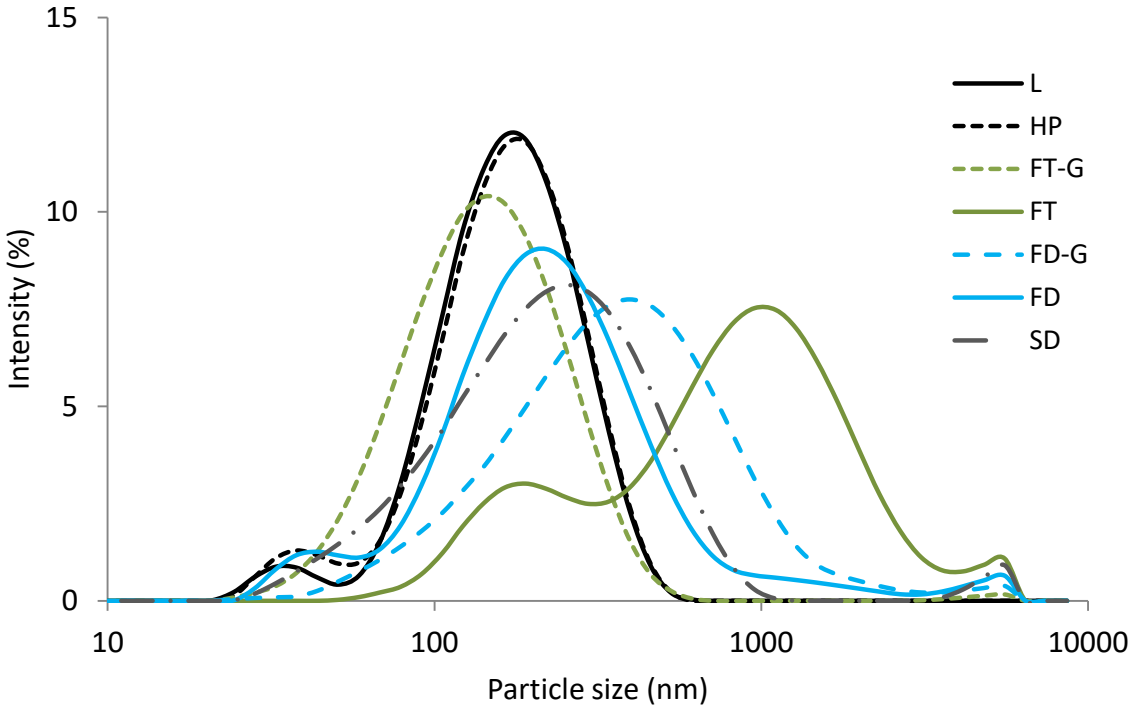
15
10
5
0
Intensity (%)
10
100
1000
10000
Particle size (nm)
L
HP
FT-G
FT
FD-G
FD
SD

Figure 1

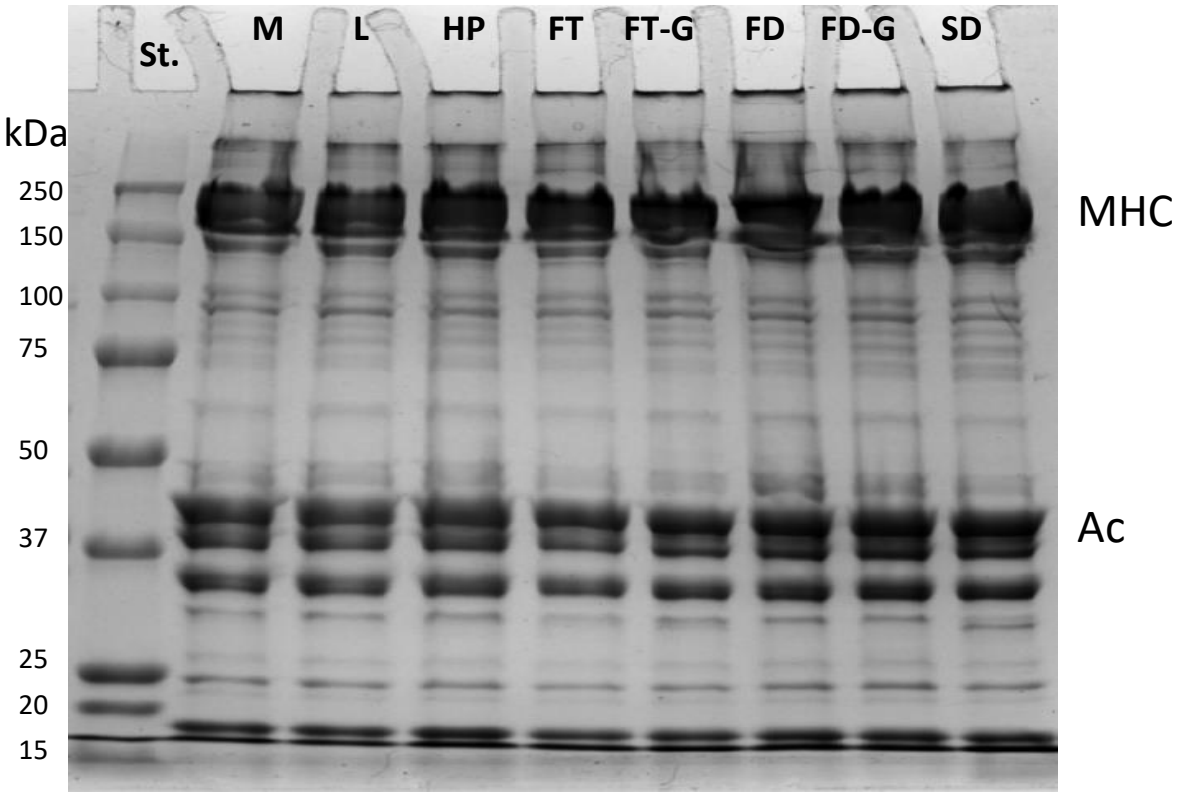

Figure 2

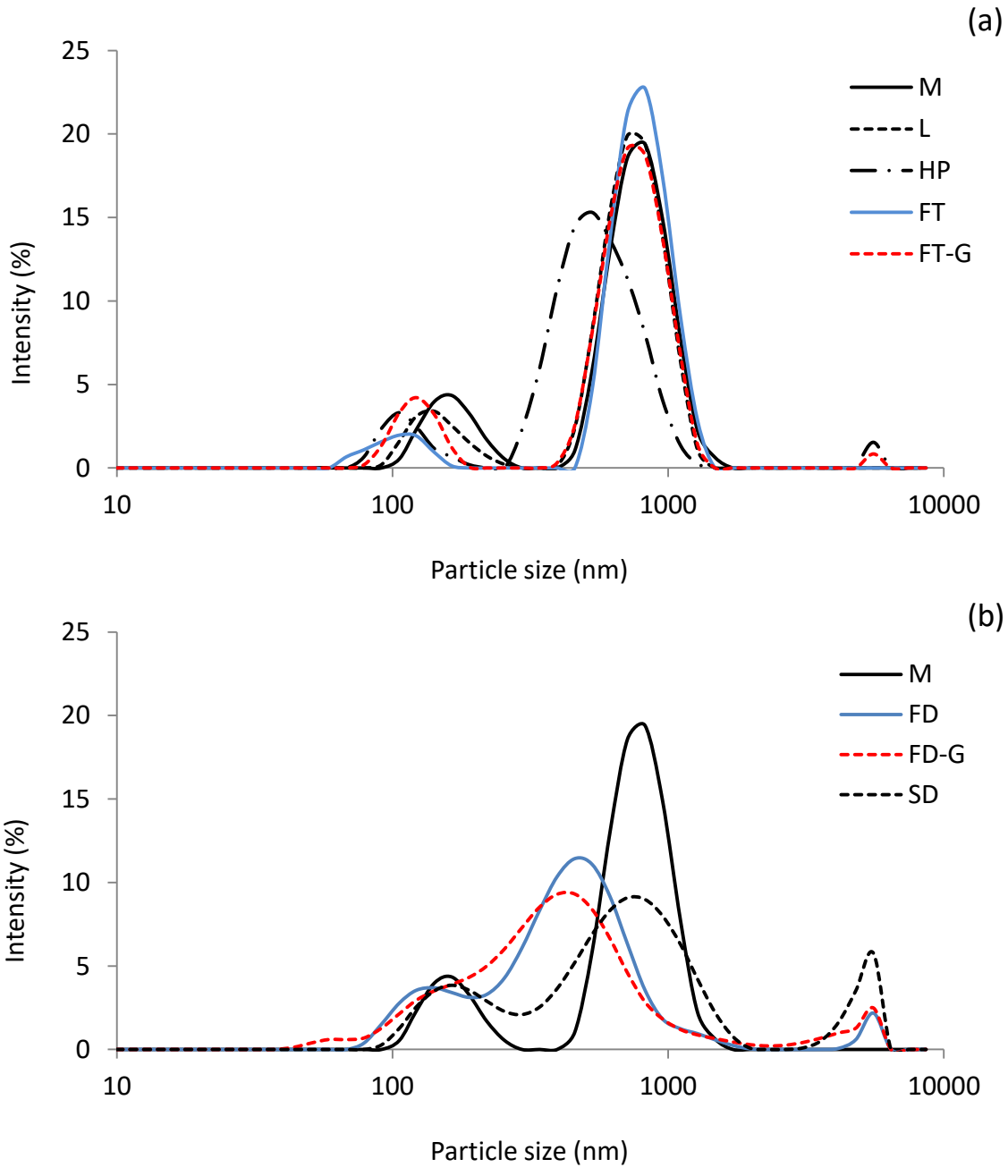
(a)
25
20
15
10
5
0
Intensity (%)
10
100
1000
10000
Particle size (nm)
M
L
HP
FT
FT-G
(b)
25
20
15
10
5
0
Intensity (%)
10
100
1000
10000
Particle size (nm)
M
FD
FD-G
SD

Figure 3

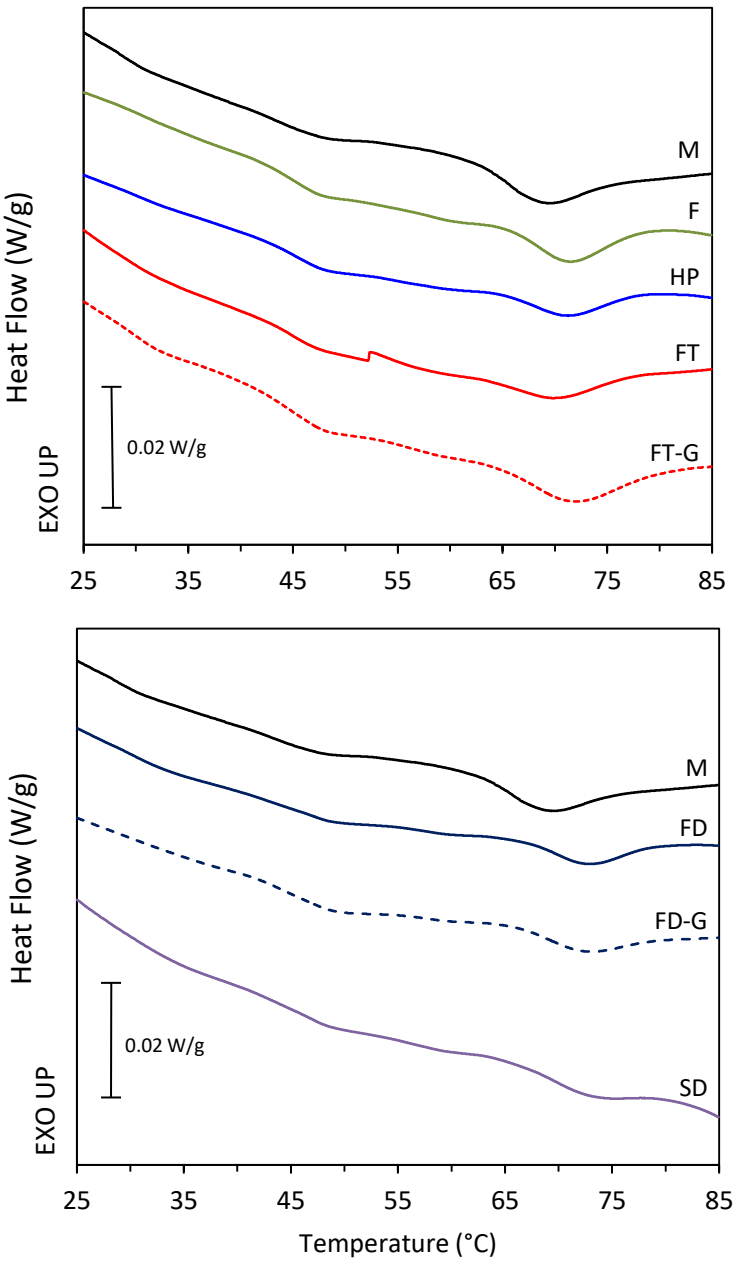
Heat Flow (W/g)
EXO UP
0.02 W/g
M
F
HP
FT
FT-G
25
35
45
55
65
75
85
Heat Flow (W/g)
EXO UP
0.02 W/g
M
FD
FD-G
SD
25
35
45
55
65
75
85
Temperature (°C)

Figure 4

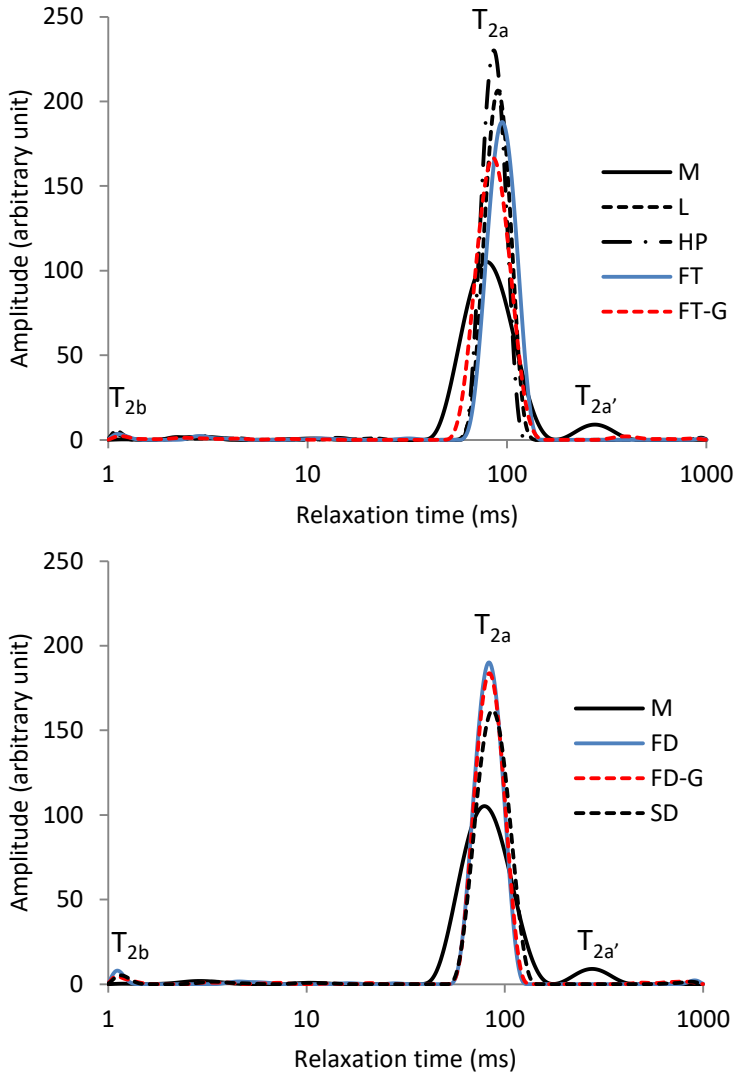
250
200
150
100
50
0
Amplitude (arbitrary unit)
T2a
T2b
T2a'
M
L
HP
FT
FT-G
1
10
100
1000
Relaxation time (ms)
250
200
150
100
50
0
Amplitude (arbitrary unit)
T2a
T2b
T2a'
M
FD
FD-G
SD
1
10
100
1000
Relaxation time (ms)

Figure 5

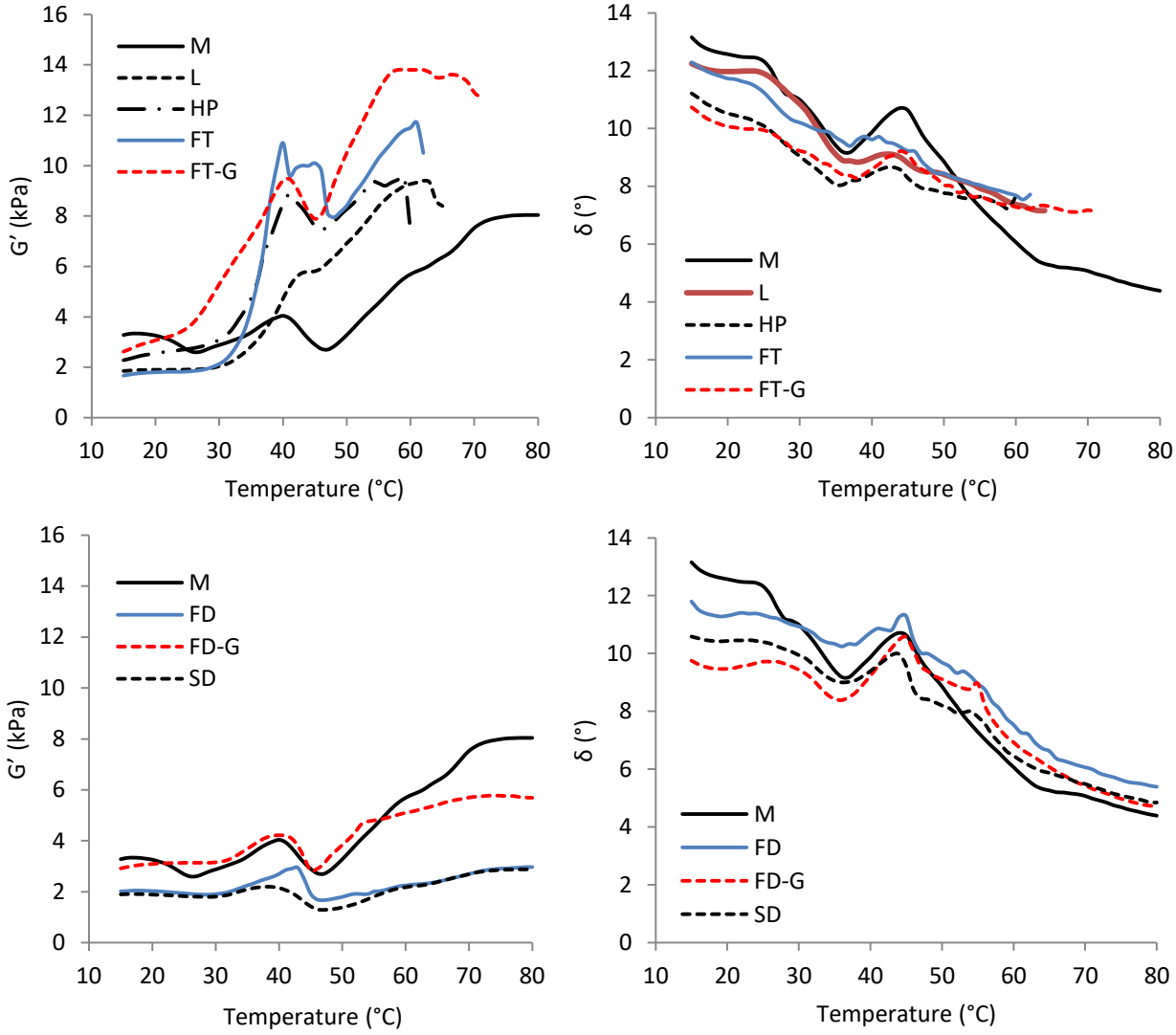
G′ (kPa)
Temperature (°C)
M
L
HP
FT
FT-G
δ (°)
Temperature (°C)
M
L
HP
FT
FT-G
G′ (kPa)
Temperature (°C)
M
FD
FD-G
SD
δ (°)
Temperature (°C)
M
FD
FD-G
SD

Figure 6

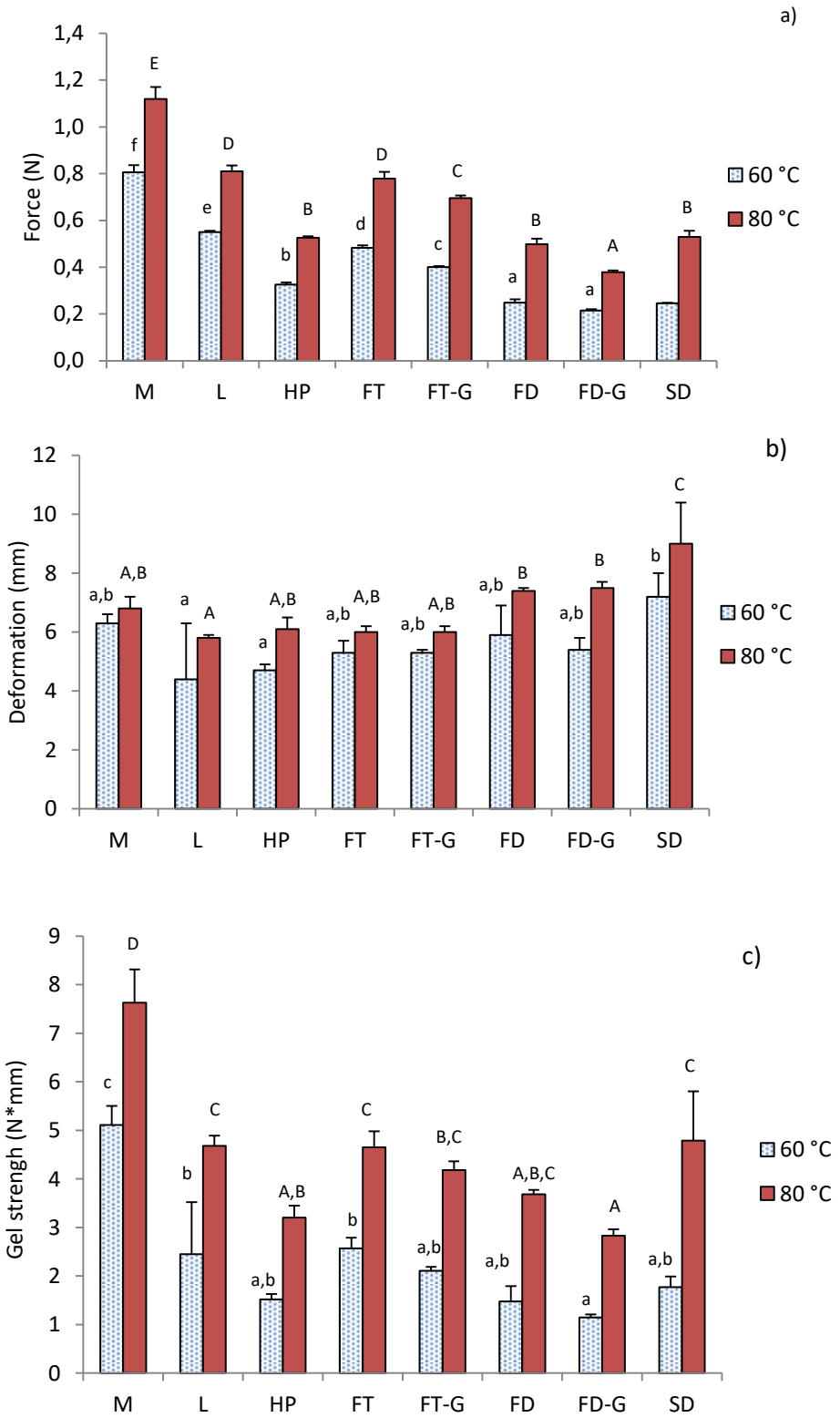
a)
Force (N)
1,4
1,2
1,0
0,8
0,6
0,4
0,2
0,0
f
E
e
D
b
B
d
D
c
C
a
B
a
A
B
M
L
HP
FT
FT-G
FD
FD-G
SD
60 °C
80 °C
b)
Deformation (mm)
12
10
8
6
4
2
0
a,b
A,B
a
A
a
A,B
a,b
A,B
a,b
A,B
a,b
B
a,b
B
b
C
M
L
HP
FT
FT-G
FD
FD-G
SD
60 °C
80 °C
c)
Gel strengh (N*mm)
9
8
7
6
5
4
3
2
1
0
c
D
b
C
a,b
A,B
b
C
a,b
B,C
a,b
A,B,C
a
A
a,b
C
M
L
HP
FT
FT-G
FD
FD-G
SD
60 °C
80 °C

Figure 7